Mar Biol (2009) 156:1559–1572
DOI 10.1007/s00227-009-1192-3

ORIGINAL PAPER

Microstructures of Antarctic cidaroid spines: diversity of shapes and ectosymbiont attachments

Bruno David · Stuart R. Stock · Francesco De Carlo · Vincent Hétérier · Chantal De Ridder

Received: 25 November 2008 / Accepted: 12 March 2009 / Published online: 12 April 2009

Abstract The echinoderm endoskeleton, located in the connective layer of the tegument, is organized into a three-dimensional mesh, the stereom. Among echinoids, the cidaroids depart from this pattern, and the shaft of the spine lacks an epidermis. Thus, the spines lack antifouling protection, allowing ectosymbionts such as bryozoans and foraminiferans to attach. This raises a question about the adaptive role of the cortical layer of the stereom. This study examined the micro- and mesostructure of the spines of 11 cidaroid species collected in the Weddell Sea and Drake Passage, and the nature of their ectosymbiont attachments. Scanning electron microscopy was used to characterize the cortex surface and X-ray micro computed tomography (μCT) to describe the symbiont attachments. Spine microstructure features provide a useful taxonomic character for distinguishing among three species in the genus *Ctenocidaris*, and challenge a previous parasitic interpretation of cortical filaments on the spines of *Rhynchocidaris triplopora*. Ectosymbiont attachments were classified as Anchoring, Molding, Cementing, or Corroding. The study suggests that some microstructure features may be protective, keeping the ectosymbionts away from the cortex and loosely attached at intervals along the shaft of the spine, while other micro-structures facilitate attachment over considerable areas of the shaft.

Communicated by J.P. Grassle.

Electronic supplementary material The online version of this article (doi:10.1007/s00227-009-1192-3) contains supplementary material, which is available to authorized users.

B. David (✉) · V. Hétérier
Biogéosciences, UMR CNRS 5561,
Université de Bourgogne, 6 bd. Gabriel, 21000 Dijon, France
e-mail: bruno.david@u-bourgogne.fr

S. R. Stock
Department of Molecular Pharmacology and Biological Chemistry, Feinberg School of Medicine,
Northwestern University, Chicago, IL 60611-3008, USA

F. De Carlo
Advanced Photon Source, Argonne National Laboratory,
Argonne, IL 60439, USA

V. Hétérier · C. De Ridder
Laboratoire de Biologie Marine, Université Libre de Bruxelles,
50 avenue F.D. Roosevelt, Bruxelles 1050, Belgium

Introduction

Echinoderm skeletal elements are unique as they are composed of high-magnesium calcite organized in a three-dimensional meshwork called the stereom. The stereom constitutes a basal apomorphy lending partial support for the monophyly of almost the whole phylum Echinodermata (only the enigmatic fossil *Arkarua* may fall below this node, see Mooi and David 1998 for details). The fine 3D microstructure of the stereom is very variable in design as in porosity, from dense imperforate stereom to coarsely open labyrinthic stereom. Different skeletal elements and different positions within a given element (plate, spine) express such variations. Stereom variations have been extensively explored by Smith (1980) for the class Echinoidea. He proposed a universally accepted classification of stereom structure that applies to all echinoderms.

The echinoderm stereom is of mesodermal origin. Although most skeletal elements occupy a superficial position, as the coronal plates and spines of echinoids, they are located beneath an epidermis. Hence, there is no direct interaction between the stereom and the external environment.

Within the Echinoidea, a major departure from the rule occurs in the order Cidaroida whose primary spines are devoid of epidermis on their shaft (Märkel and Röser 1983b). Cidaroid spines classically form internally, but, contrary to other echinoids, their shaft loses most of its epidermis once the growth of the spine is complete. Only the basal part, where muscles and collageneous fibers insert, retains an epidermis. This characteristic, apomorphic for cidaroids, is important in the ecology of the clade.

Because an epidermis covers the spines of most echinoids, ectosymbiotic interactions are restricted to just a few parasites (Vaitilingon et al. 2004) and mutualist non-attached hosts (Alvarado 2008). Contrasting with this condition, the cidaroid spines are bare calcium carbonate rods without any antifouling protection. This allows various ectosymbionts to settle (Hétérier et al. 2004; Linse et al. 2008). Cidaroid spines are generally structured in three layers: (1) an internal core, or medulla (made of open labyrinthic stereom, sensu Smith 1980); (2) a dense intermediary layer of radiating septa (made of rectilinear stereom); (3) a still more dense outer cortex (made of irregular perforate to imperforate stereom). The boundary between the two internal layers is not always sharp, and the thickness of the transition zone varies. The cortex is generally sharply delimited. In some cases, the cortex itself can be differentiated into two layers (Fell 1954; Märkel and Röser 1983a). Spines can be considered at different scales that of the size and gross morphology of the spines (macrostructures); that of serrations, bumps, ridges, and thorns ornamenting the spines (mesostructures); and that of the stereom trabeculae (microstructures). Along the spine shaft, the mesostructures are most often formed by the cortex alone (Mortensen 1928). Only the larger mesostructures may incorporate some open stereom from the underlying layer. At the surface of the shaft, microstructures occur in a wide variety of shapes ranging from short, acute microspines, to fine cross-connecting trabeculae, or to tiny more or less interconnected umbrellas.

The variety of stereom structures, the diversity of ectosymbionts (e.g. up to 60 morphological types colonize *Ctenocidaris spinosa*, Hétérier et al. 2004), and the taxonomic richness of Cidaroida (about 150 living species) can be set as three points corresponding to the vertices of a triangle. In this triangular frame, three axes deserve exploration. (1) Stereom—Taxonomy: Could stereom structures provide additional taxonomic characters? (2) Stereom—Ectosymbionts: How do stereom structures influence the settlement of ectosymbionts? (3) Ectosymbionts—Taxonomy: What is the specificity of ectosymbionts for particular cidaroid species? The present paper addresses the first two points, since the question of symbiont specificity requires more investigation that isl beyond the scope of this study.

Cidaroids are easily distinguished from other regular echinoids as they have a robust test with large interambulacral plates bearing a single primary tubercle. Cidaroid tests are quite similar in shape and plate pattern, so the systematics of the clade mostly relies on the gross morphology of spines (Mortensen 1928). However, the systematics of cidaroids is far from clear, and the relationships between genera and species are conjectural (David et al. 2005a). Significant improvements will definitely require molecular phylogenetic approaches (Lockhart et al. 2003), but the addition of new morphological characters, such as stereom microstructures, may help to elucidate some taxonomic questions.

The second axis above deals with the adaptive significance of the superficial layers of the stereom. Do cidaroids develop specific structures to hinder or, conversely, help the settlement of symbionts? Similarly, how do ectosymbionts benefit or not from the diverse structures of the spines? Such issues can be addressed at all scales: micro-, meso-, and macrostructures. Earlier reports have shown that both the size (macroscale) and the ornamentation (mesoscale) of the spine influence the diversity of the community of symbionts (Hétérier et al. 2004). But such studies remain rare, and none deals with the microstructures of the spines due to technical difficulties of investigation.

To investigate those two issues, and to keep the environmental and phylogenetic parameters as similar as possible, the present study focused on the subclade Ctenocidarinae, which comprises exclusively Antarctic and sub-Antarctic species. Ctenocidarinae display a broad disparity of spine morphologies (Mooi et al. 2000), as well as a considerable diversity of ectosymbionts (Gutt and Schickan 1998; Hétérier et al 2008). In the Austral Ocean, they are represented by 21 species belonging to five genera (David et al. 2005b).

Materials and methods

A set of 11 Antarctic cidaroid species, representing high morphological diversity of spines and the five genera of Ctenocidarinae, were examined (Table 1). All collected specimens came from recent oceanographic cruises, and were collected with an Agassiz trawl (except *Austrocidaris canaliculata*, which was from an historical collection at the Museum of Paris). Spines were directly removed from specimens preserved in ethanol, and then slowly dried at ambient temperature before examination. The studied spines were randomly taken on the apical or on the oral region, but all were covered, at least partially, by symbionts.

The spine macro-, meso-, and microstructures as well as spine ectosymbionts were studied using three complementary techniques. Classical optical microscopy identified

Table 1 List of studied taxa

Species author	Analysis	Latitude longitude	Depth (m)	Regions
Aporocidaris milleri (A. Agassiz, 1898)	µCT/1	70°93S 10°54W	290	Kapp Norvegia
Austrocidaris canaliculata (A. Agassiz, 1863)	µCT/1	?	?	Drake passage
Ctenocidaris geliberti (Koehler, 1912)	µCT/1	62°10S 58°25W	200	South Shetlands
Ctenocidaris perrieri Koehler, 1912	µCT/4 M/10	70°52S 10°28W	240	Kapp Norvegia
Ctenocidaris rugosa (Koehler, 1926)	µCT/1	72°51S 19°10 W	450	East Weddell Sea
Ctenocidaris speciosa Mortensen, 1910	µCT/1 M/10	73°28S 22°30W	1,680	East Weddell Sea
Ctenocidaris spinosa (Koehler, 1926)	µCT/1 M/10	71°09S 12°26W	360	Kapp Norvegia
Notocidaris hastata Mortensen, 1909	µCT/1	61°34S 58°12W	420	South Shetlands
Notocidaris lanceolata Mooi, David, Fell and Choné, 2000	µCT/2	71°90S 12°09W	330	Kapp Norvegia
Notocidaris platyacantha (H.L. Clark, 1925)	µCT/1	66°53S 73°15E	500	Prydz Bay
Rhynchocidaris triplopora Mortensen, 1909	µCT/2	72°51S 19°11W	390	East Weddell Sea

First column indicates species name and author. Second column gives number of specimens analyzed by microtomography (µCT/n), or used for morphometry (M/10). Last three columns provide information about geographic origin of specimens

ectosymbionts and assessed spine macro- and mesostructures. Scanning electronic microscopy (SEM) explored the surface of the spines at the scales of meso- and microstructures. X-ray micro-computed tomography (µCT) imaged the close spatial relationships between spines and symbionts and provided 3D microstructural data. This non-destructive technique was the only way to assess the spine–symbiont topological interaction without alteration of the system. Laboratory (microfocus tube-based) µCT and synchrotron µCT were used with the spine axes oriented parallel to the tomography rotation axis. The microfocus µCT system (Scanco MicroCT-40, Scanco Medical GBMH) was used to study spines whose diameters were too large for synchrotron µCT and to survey smaller spines for suitability for imaging at higher spatial resolution with synchrotron X-radiation. The Scanco MicroCT-40 imaging parameters used were 70 kVp X-ray tube potential and reconstruction with either 6- or 8-µm volume elements (voxels), depending on the specimen diameter. Synchrotron µCT was performed at bending magnet station 2-BM at the Advanced Photon Source (APS); the system is described elsewhere (Wang et al. 2001). The spines were imaged (unless otherwise noted) with 21.2 keV X-ray photons using a 1 K × 1 K CCD camera coupled to a cadmium tungstate single crystal scintillator though a 2.5× optical lens (except for a few larger specimens, noted below, which were imaged with a 1.25× lens). The reconstructions were with isotropic volume elements (i.e. cubic voxels with equal dimensions in all three directions); with the 2.5× lens, the voxel size was 2.8 µm (with the 1.25× the size was twice as large).

The µCT observations required no specific preparation of the spines. For the SEM, a gentle cleaning and removal of the symbionts were done on a second set of spines. The identification of symbionts was done by light microscopy as precisely as possible, generally at the genus level. A single spine per species was prepared for SEM, and one to four was observed by µCT (Table 1).

Three species—*C. perrieri*, *C. speciosa* and *C. spinosa*—were more extensively investigated because of their taxonomic relationship. A morphometric appraisal was undertaken for their apical spines. For each species, two interambulacral primary spines were sampled in distinct growth zones (David and Mooi 1999) on the apical side on 10 specimens (totally 20 spines per species). Each spine was gently cleaned of symbionts for numerical capture, binarisation, and measurements of 11 morphological parameters. The first seven parameters are related to the size of the structures and were measured on digital images of the spines using Optimas®. The last four correspond to

ratios, which are relatively independent of size. Together, these parameters described the size and shape of the spines (supplementary table S1). Measurement errors were estimated from two replicates using the method of Bailey and Byrnes (1990) and were low (supplementary table S1). A factorial analysis was performed to build the morphospace of the 60 apical spines of the three species. A complementary quantitative investigation of symbiont coverage was done on another set of 60 spines sampled from the same specimens. This approach used two criteria: (1) the level of spine coverage estimated using four classes (0–25%, 25–50%, 50–75%, 75–100%); (2) the abundance of symbiotic specimens ranked in four categories (0: no symbiont; 1: few symbionts; 2: abundant symbionts; 3: very abundant symbionts). Both criteria were recorded on the proximal and distal part of spines, thus leading to a set of four variables allowing computation of Mahalanobis distances between the three investigated species. Factorial and discriminant analyses were performed with the package Statistica 6.1.

Results

Meso- and microstructure of spines

The spine-mesostructures observed in Ctenocidarinae fall into three main categories. (1) Barely distinct structures correspond to differential stereom density at the surface of the spine (e.g. the cellular pattern observed in *C. geliberti*). Such superficial patterns are the mesoscale expression of microstructural differences. (2) Local structures such as thorns (e.g. in *C. perrieri*, Fig. 1a) or bumps (e.g. in *C. rugosa*, Fig. 1b) of various sizes. They can be randomly distributed on the surface of the spine or arranged in regular rows. Bumps are more or less elongated and symmetrical. Thorns are more or less oblique, curved, twisted, and sharp. (3) Longitudinal structures such as folds (e.g. in *A. canaliculata*, Fig. 1c), ridges or crests (e.g. in *N. hastata*, Fig. 1d) that occupy various lengths of the spine. Mesostructures generally involve only the cortex of the spine, but they can also encompass the intermediary layer (e.g. the thorns of *C. spinosa*). At a smaller scale, microstructures are direct expressions of stereom trabeculae of the cortex, which can project more or less from the body of the spine. They are blunt (e.g. the "nails" observed in *C. geliberti*), thick (e.g. the serrations of *N. hastata*), or more or less sharp microspines (e.g. *C. perrieri*, Fig. 1e), and, at the extreme, long spikes or filaments (*R. triplopora*).

Among the 11 investigated Antarctic species, most of the observed microstructures correspond to microspines that differ in size, shape, orientation and position on the shaft. The mesostructures belong to various types (bumps, ridges, serrations, thorns) which were used below to rank the species from less to more ornamented.

The glossy oral spines of *Notocidaris lanceolata* bear no ornamentation with the exception of their lateral indented wings, which can be considered macrostructures. The cortex is very dense and has a smooth outer surface.

Faint ornamentation exists on the spines of *C. geliberti*. Optical observation shows a regular array of more or less circular beige cells separated by whitish walls. The μCT data show that both cells and walls correspond to a thick, well-differentiated cortex. The cells appear to match dense, imperforate stereom, while the walls likely correspond to parts of the outer cortex consisting of small trabeculae fused at their abaxial margins, i.e. they look like an array of small, touching nails (Fig. 2a).

Austrocidaris canaliculata displays irregular longitudinal folds, conspicuous at the magnification of a binocular microscope, and of fibrous aspect (Fig. 1c). The μCT data show, however, that the cortex forming those mesostructures is hardly differentiated from the underlying intermediary layer and consists of irregular perforate stereom. Actually, the cortex is almost absent in some places and thicker at others, with a spongy appearance with cavernous holes. At the microstructural scale, the surface of *A. canaliculata* spines appears rugose and wrinkled, but devoid of microspines.

Ornamentation with longitudinal structures similar to that observed in *A. canaliculata* occurs in *Notocidaris hastata* (Fig. 1d). This ornamentation is intermediate between meso- and microstructures. Robust and rather large, thick microspines (serrations) cover the surface of the shaft. These serrations are highly oblique, and look like small balloons floating outside the spine in μCT slices (Fig. 2b). At several irregularly spaced locations, longitudinal ridges are present, formed by fusion of extended serrations (at the optical scale, they appear glued together). The cortex, as observed in μCT, is a continuation of the underlying stereom with thicker, more massive elements. All this makes the surface of the shaft very rough and traps many sediment particles around the spine.

Rounded bumps are irregularly distributed around the shaft of *Aporocidaris milleri*. These bumps contain dense, weakly perforated stereom. Similar mesostructural bumps, more or less elongated into small thorns and slightly oblique, occur in *Ctenocidaris rugosa* (Fig. 1b). As in *A. milleri*, they are extensions of a dense cortex (Fig. 2c). *A. milleri* bears rather small microspines, and the μCT data show that they radiate orthogonal to the shaft surface and are regularly distributed. They are not developed, or only weakly so, on the bumps. The cortex of *C. rugosa* develops rather similar microspines, although a bit smaller.

Notocidaris platyacantha has very specific flattened primary spines almost devoid of ornamentation. Those spines

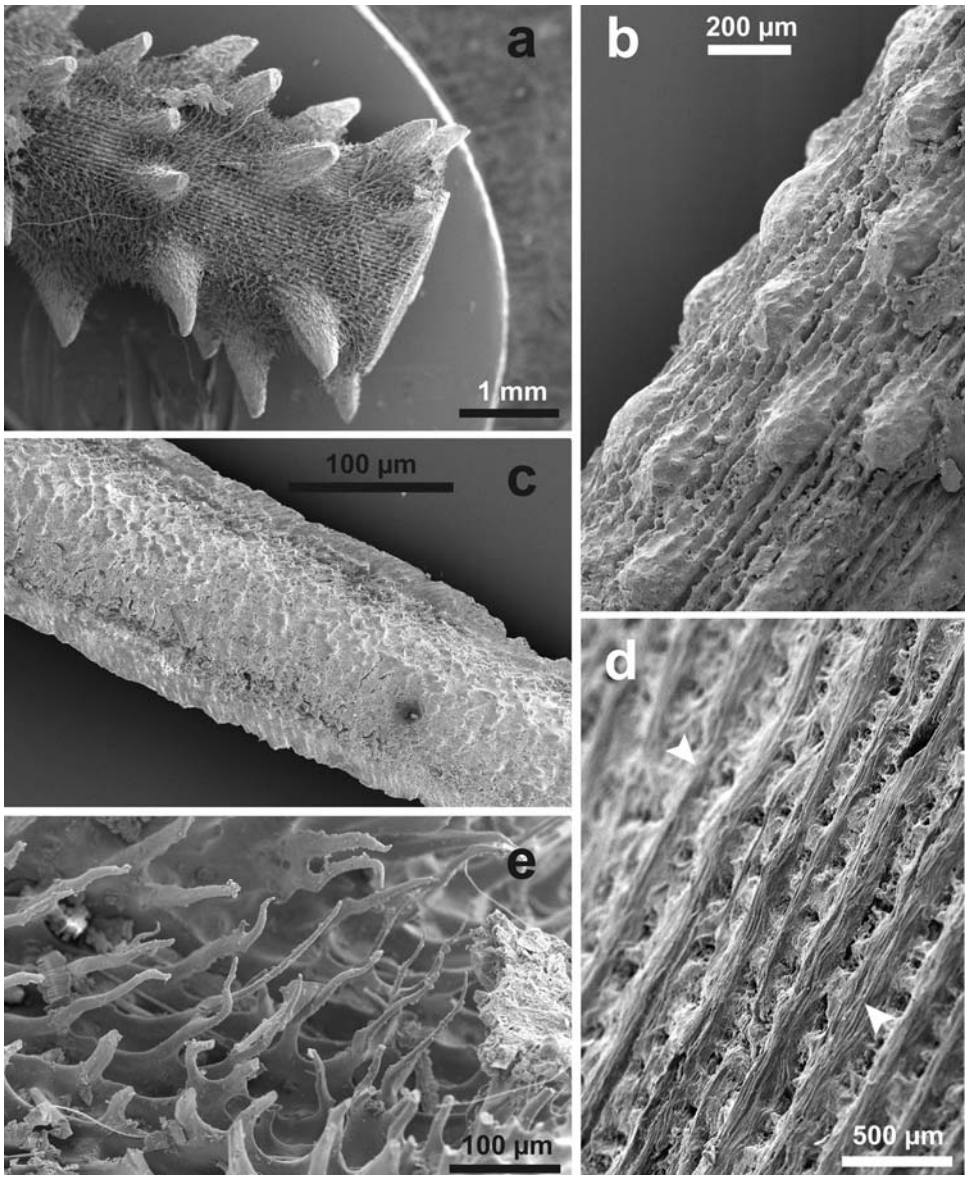

Fig. 1 SEM views of meso- and microstructures of spines. **a** Large thorns on a *Ctenocidaris perrieri* spine. **b** Bumps on a *C. rugosa* spine. **c** Longitudinal folds on an *Austrocidaris canaliculata* spine. **d** Ridges (*arrows*) on a *Notocidaris hastata* spine. **e** Microspines on *C. perrieri*

bear narrow lateral extensions, which are integral to the intermediary layer or a thickening of the well-differentiated cortex (Fig. 3b). Sparsely distributed small thorns may occur at some places rarely. They consist exclusively of cortex. The internal core occupies most of the spine, the intermediary layer being more reduced than in other species. The cortex of *N. platyacantha* also develops small, regularly spaced, microspines, almost identical to those of *C. rugosa*.

Ctenocidaris perrieri, *C. speciosa* and *C. spinosa* spines develop large thorns. In *C. perrieri*, the cortex is difficult to distinguish and is almost reduced to a single stereom lamella of the same thickness as the lamina of the underlying layer. Despite this thinness, the thorns grow as solid extensions of the cortex from which they are largely derived (Fig. 2d). Even if completely grown thorns are not completely solid, they generally consist of rather dense stereom and are almost straight. They are high and sharp, and there can be up to five around the spine circumference. In *C. speciosa* and *C. spinosa*, a thin, continuous, clearly visible cortex covers the entire thorns. Therefore, the thorns integrate the stereom fabric of the internal layer. Moreover, the transition between the internal core and the intermediary layer is gradual and difficult to discern (particularly in *C. spinosa*). The thorns are very long, sinuous and numerous and surround the spine circumference in *C. spinosa* (up to 11 within the ~3.5 mm of spine length surveyed by synchrotron µCT) (Fig. 2e). They are squat and closer to large bumps in *C. speciosa* (up to eight in the 3.4 mm surveyed) (Fig. 2f). In both *C. speciosa* and *C. spinosa*, the whole spine digitates more or less strongly. The difference is more a matter of degree than of kind, while in *C. perrieri*, thorns

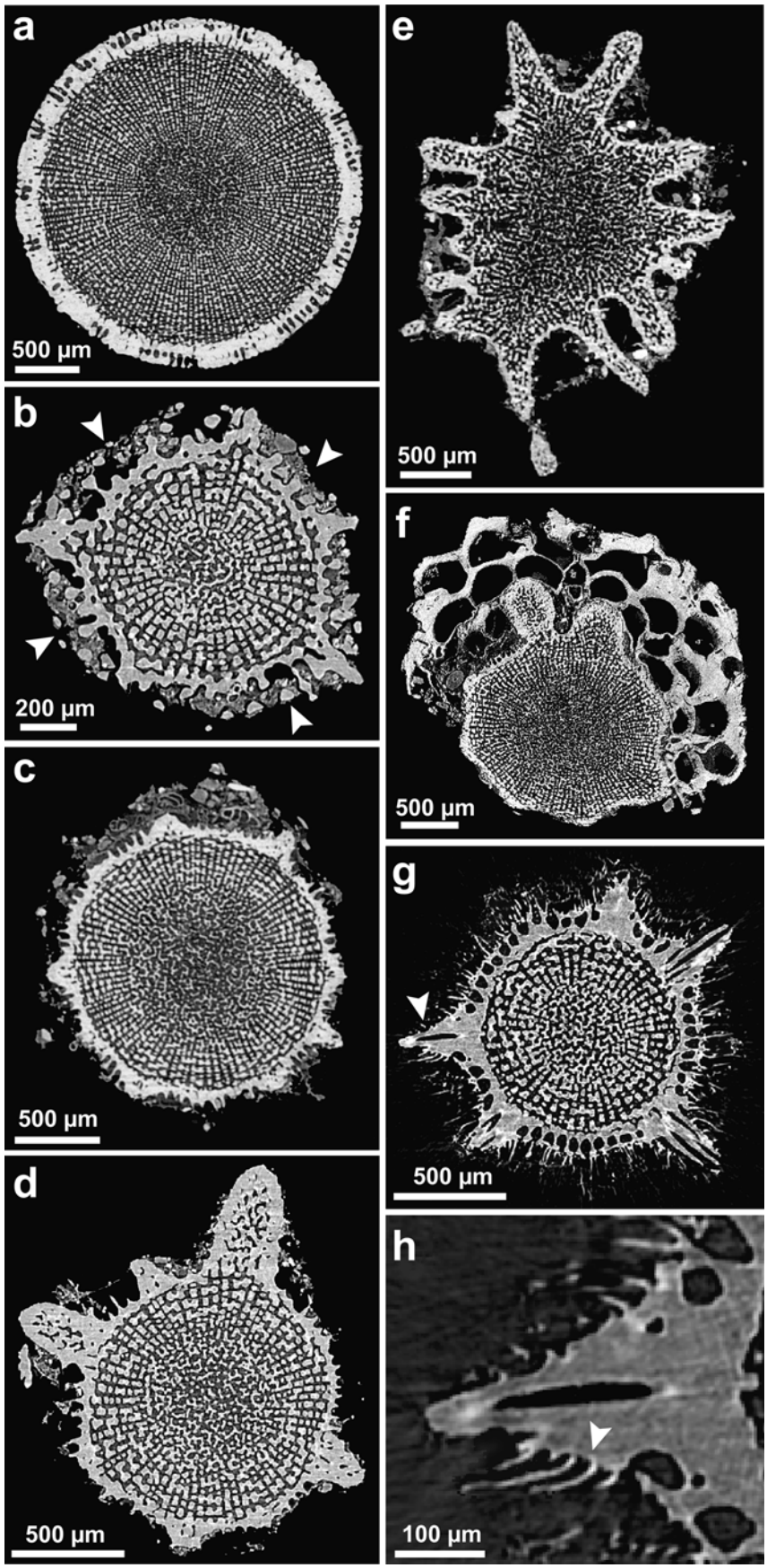

Fig. 2 Synchrotron µCT slices of spines aligned perpendicular to the spine axis. They illustrate various micro- and mesostructures of the spines. **a** *Ctenocidaris geliberti*. **b** *Notocidaris hastata*. Many sedimentary particles are trapped around the shaft (*arrows*). **c** *C. rugosa*. **d** *C. perrieri*. **e** *C. spinosa*. **f** *C. speciosa*. **g** *R. triplopora*, entire spine. **h** *R. triplopora*, four times enlargement of the thorn indicated by an *arrow* in **g**, showing details of the filament anchorage (*arrow*). In all slices, the lighter the pixel, the more heavily attenuating the corresponding voxel. (**a**, **c**, **e** reconstructions with ~5.6 µm voxels) (**b**, **d**, **f**–**h** reconstructions with ~2.8 µm voxels)

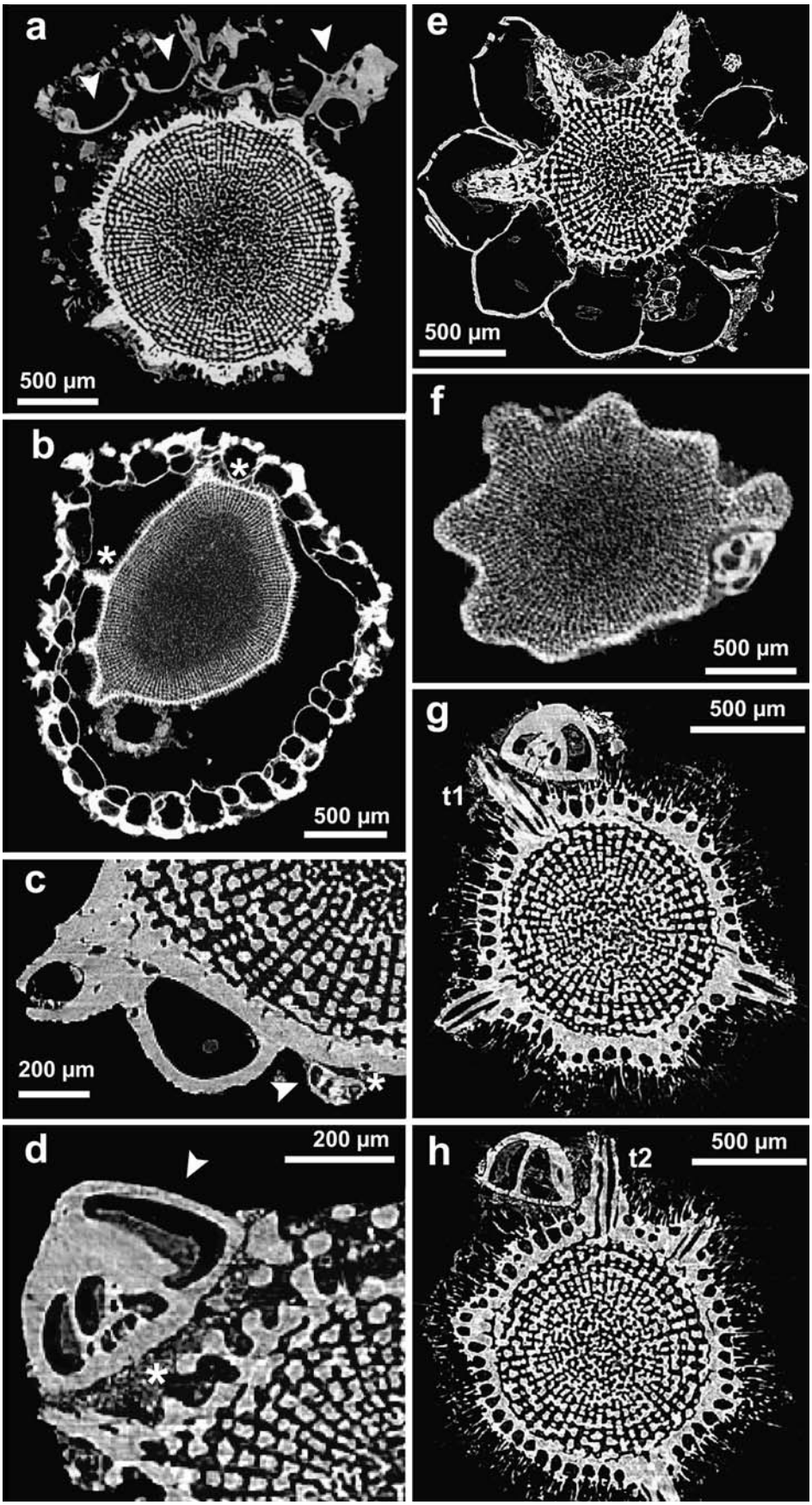

Fig. 3 Synchrotron µCT slices illustrating various ectosymbiont attachments by anchoring on cidaroid spines. **a** The bryozoan *Arachnopusia* sp. 2 (*arrows*) on *Ctenocidaris rugosa*. **b** The bryozoan *Arachnopusia* sp. 1 anchored on the spine of *Notocidaris platyacantha* at a few points (*asterisks* show two of them). **c** portion of synchrotron µCT slice showing the foraminifer *Cibicides* sp. (*arrow*) on *N. lanceolata.* **d** Portion of synchrotron µCT slice showing the foraminifer *Cibicides* sp. (*arrow*) on *N. hastata*. In **c** and **d**, *asterisks* indicate sedimentary particles wedged underneath the foraminifers. **e** The bryozoan *Chaeperiopsis cervicornis* on *C. perrieri*. **f** Scanco MicroCT-40 µCT slice showing a large foraminifer wedged between the bumpy thorns of *C. speciosa.* **g**, **h** A large *Cibicides* between the thorns of *Rhynchocidaris triplopora.* Frames **g** and **h** show the same foraminifer in slices 0.14 mm apart abutting two different thorns (labeled t1 and t2). (**a**, **c–e**, **g**, **h** reconstructions with ~2.8 µm voxels) (**b** reconstruction with ~8 µm voxels) (**f** reconstruction with 6 µm voxels)

are, as most ornamental mesostructures in other species, peripheral cortical extensions. At the microstructural scale, the cortex of *C. perrieri* is covered with regularly distributed sharp microspines, including at the base of the large thorns. *Ctenocidaris speciosa* shows sparse small microspines that seem restricted to gently undulating parts of the circumference or to depressions between bumpy thorns. Rather similar microspines also exist in *C. spinosa*, but they also occur on the thorns and are less sparse and more oblique than those of *C. speciosa*.

The cortex of *Rhynchocidaris triplopora* combines large acuminate thorns with umbrella-shaped trabeculae (Fig. 2g). Both of these structures are perpendicular to the shaft. The thorns are not solid but made of perforated stereom, the perforations being canal-like in the direction of the thorn. At some places, the perforations open at the tip of the thorns, which appears as the thorn is made of coalescent huge spikes. At other places, thorns are more robust, but their surface is always irregular. The umbrella-shaped trabeculae rise from the basal part of the cortex. They are regularly distributed and generally fused at their tops, thus isolating small alveolate cavities just below the surface of the shaft. In addition, *R. triplopora* displays filaments raising far away the main surface of the spine (Fig. 2h). Those filaments are very thin, some anastomosed, and clearly connected to the cortex all around the shaft, including on thorns. Optical observations confirm that the filaments are calcite-like and transparent.

Symbiont attachments

The μCt survey provided precise information on the intimate physical relationships between a variety of symbionts (foraminifers, sponges, hydrozoa, annelids,…) and the various micro- and mesostructures of the spines. Different levels of interaction between the structures and the symbionts are presented from the weakest to the strongest encrustations and a summary of the different cases is given (Table 2).

Anchoring

In this type of attachment, there is limited interaction between the symbiont and the spine. The symbiont appears fixed at only a few points, or just extends along the spine.

A bivalve byssus provides a good example of classical anchoring. *Lissarca notorcadensis* firmly grips the rather smooth shaft of *C. geliberti*, but without altering the cortex of the spine. Hydrozoans *(Filellum* sp.) do the same in *C. perrieri*. It is also the case, although to a lesser extent, in *A. canaliculata* (spirorbid polychaetes fixed by a whorl at one point, appear to float above the spine elsewhere), and in

Table 2 Four types of ectosymbiont attachment to spines of 11 Antarctic cidaroid species, and taxonomic identity of the symbionts

Type of attachment	Hosts	Symbionts
Anchoring	*Austrocidaris canaliculata*	Spirorbidae (P)
		Cibicides sp. (F)
	Ctenocidaris geliberti	*Lissarca notorcadensis* (Bi)
	Ctenocidaris perrieri	*Cibicides* sp. (F)
		(*Filellum* sp.) (H/T)
		Chaperiopsis cervicornis (Br/C)
	Ctenocidaris rugosa	*Arachnopusia* sp. 2 (Br/C)
		Foraminifera
	Ctenocidaris speciosa	Foraminifera
	Notocidaris hastata	*Cibicides* sp. (F)
	Notocidaris lanceolata	*Cibicides* sp. (F)
	Notocidaris platyacantha	*Arachnopusia* sp. 1 (Br/C)
	Rhynchocidaris triplopora	*Cibicides* sp. (F)
Molding	*Aporocidaris milleri*	*Osthimosia* sp. 1 (Br/C)
	Ctenocidaris perrieri	*Smittina obicullata* (Br/C)
	Ctenocidaris speciosa	*Osthimosia* sp. 1 (Br/C)
Cementing	*Austrocidaris canaliculata*	Bryozoa Cheilostomata
	Ctenocidaris perrieri	*Chaperiopsis cervicornis* (Br/C)
	Notocidaris lanceolata	*Micropora* sp. (Br/C)
		Osthimosia sp. 2 (Br/C)[a]
		Spirorbidae (P)
Corroding	*Notocidaris lanceolata*	*Cibicides refulgens* (F)

Bi Bivalvia, *Br/C* Bryozoa Cheilostomata, *F* Foraminifera, *H/T* Hydrozoa Thecata, *P* Polychaeta

[a] The genus name is uncertain for *Osthimosia* sp. 2

C. rugosa with a bryozoan (*Arachnopusia* sp. 2) (Fig. 3a). This kind of interaction is especially well illustrated by the bryozoan (*Arachnopusia* sp. 1) encircling the spine of *N. platyacantha* (Fig. 3b). The symbiont was far away from the spine, enclosing a space, and was fixed at only three or four points, particularly on thorns.

The situation, where the symbiont is not actually attached to the spine but appears to lie across it, is often encountered with foraminifers. This is illustrated by specimens of *Cibicides* sp. observed in *N. lanceolata* with some sedimentary particles wedged underneath, but closer examination reveals that they can be anchored at few points (Fig. 3c). Other foraminifers in this position have been observed in *A. canaliculata*, *N. hastata, C. rugosa, C. perrieri*, and *C. speciosa*. For example, a small *Cibicides* sp. is trapped between the serrations; a large one sits on mud retained by the serrations (Fig. 3d). The large bryozoan *Chaperiopsis cervicornis* settled on *C. perrieri* provides a spectacular example of a weak interaction between the structures of the spine and the symbiont. The huge zooecia sit side by side in a single layer that surrounds the shaft whatever the underlying structure: some abut a large thorn; others are astride a thorn (Fig. 3e). The basal walls of the zooecia are extremely thin and probably not mineralized. They do not fit the microstructures of the spine, but just surround the largest thorns. In a similar way, the large thorns of *C. speciosa*, *C. spinosa*, and *R. triplopora* offer support for the symbionts to grip, to lean against, or to be pinned between (large foraminifers in *C. speciosa*, Fig. 3f, and *R. triplopora* in Fig. 3g, h). They also have shapes that tend to catch masses of sedimentary particles as well as small organisms.

Molding

In several cases, the symbionts closely follow the outline of the spine down to the microspines. In *A. milleri*, the basal wall of bryozoan zooecia (*Osthimosia* sp. 1) closely follows the villi formed by the microspines (Fig. 4a). Laterally the same bryozoan undulates at the same wavelength as the microspines do, but the open space is a bit larger. In such cases, the mineral part of zooids never seems to contact the spine, but the basal part of the symbiont is isomorphic with the spine. At other places, the symbiont does not follow the outline of the spine. A similar situation, illustrating all degrees of molding, exists with another bryozoan (*Smittina obicullata*) on *C. perrieri*, the symbiont being alternatively closer to or farther away from the spine. The bryozoan *Osthimosia* sp. 1 has thin but mineralized basal walls that closely fit the bumpy thorns of *C. speciosa*, but this molding does not extend to the scale of the microspines (Fig. 4b) and therefore illustrates an intermediary case between molding and anchoring.

Cementing

Cementing refers to relatively wide ranging contact between mineralized parts of the symbiont and the cortex of the spine. The encrustation of the symbiont can be nearly perfect as illustrated by different species of bryozoans (*Micropora* sp. and *Osthimosia* sp. 2) settled on the glossy spines of *N. lanceolata* (Fig. 4c, d). In these cases, the basal walls of zooecia are almost perfectly fused with the cortex. In *Osthimosia* sp. 2, this basal wall appears considerably thinner than the other sides of the zooecium. A spirorbid tube provides another case of strong cementing on the same species (Fig. 4e). An extreme case of cementing is illustrated by bryozoans (Cheilostomata) installed on the irregular cavernous cortex of *A. canaliculata* (Fig. 4f). The boundary between bryozoans and the shaft of the spine is hardly discernible on µCT pictures, especially because the bryozoan colonies tend to adopt the swollen shape of the cortical folds. The bryozoans appear thus in perfect continuity with the spine, almost mimetic of the mesostructures, although they are clearly distinguishable by their color in optical images. To a lesser extent, cementation can complement molding in some cases e.g. with a bryozoan (*Chaperiopsis cervicornis*) settled on *C. perrieri*, particularly at the level of thorns, but also on a few microspines.

Corroding

Physical alteration of an *N. lanceolata* spine is probably present under the foraminifer *Cibicides refulgens.* The cortex of the spine is very uniform around its perimeter but becomes much thinner and disappears completely under the middle part of the foraminifer (Fig. 5a). In addition, the foraminifer is inserted into a lateral extension, altering the spine's microstructure (Fig. 5b).

Symbiont stacking

In many cases, different kinds of symbionts are stacked one atop the others, their interactions corresponding mostly to anchoring: foraminifer on spirorbid as in *A. canaliculata* (Fig. 5c); foraminifer under or on bryozoans as observed in *C. perrieri* or *C. speciosa* (Fig. 5d, 4b); bryozoan on bryozoan as in *C. perrieri*.

Ctenocidaris perrieri, *C. speciosa* and *C. spinosa* comparisons

The morphological investigation of *C. perrieri*, *C. speciosa* and *C. spinosa* demonstrates that the apical spines of *C. perrieri* and *C. spinosa* are almost indistinguishable in gross morphology, while those of *C. speciosa* are different (Fig. 6). The two first axes of the factorial analysis account

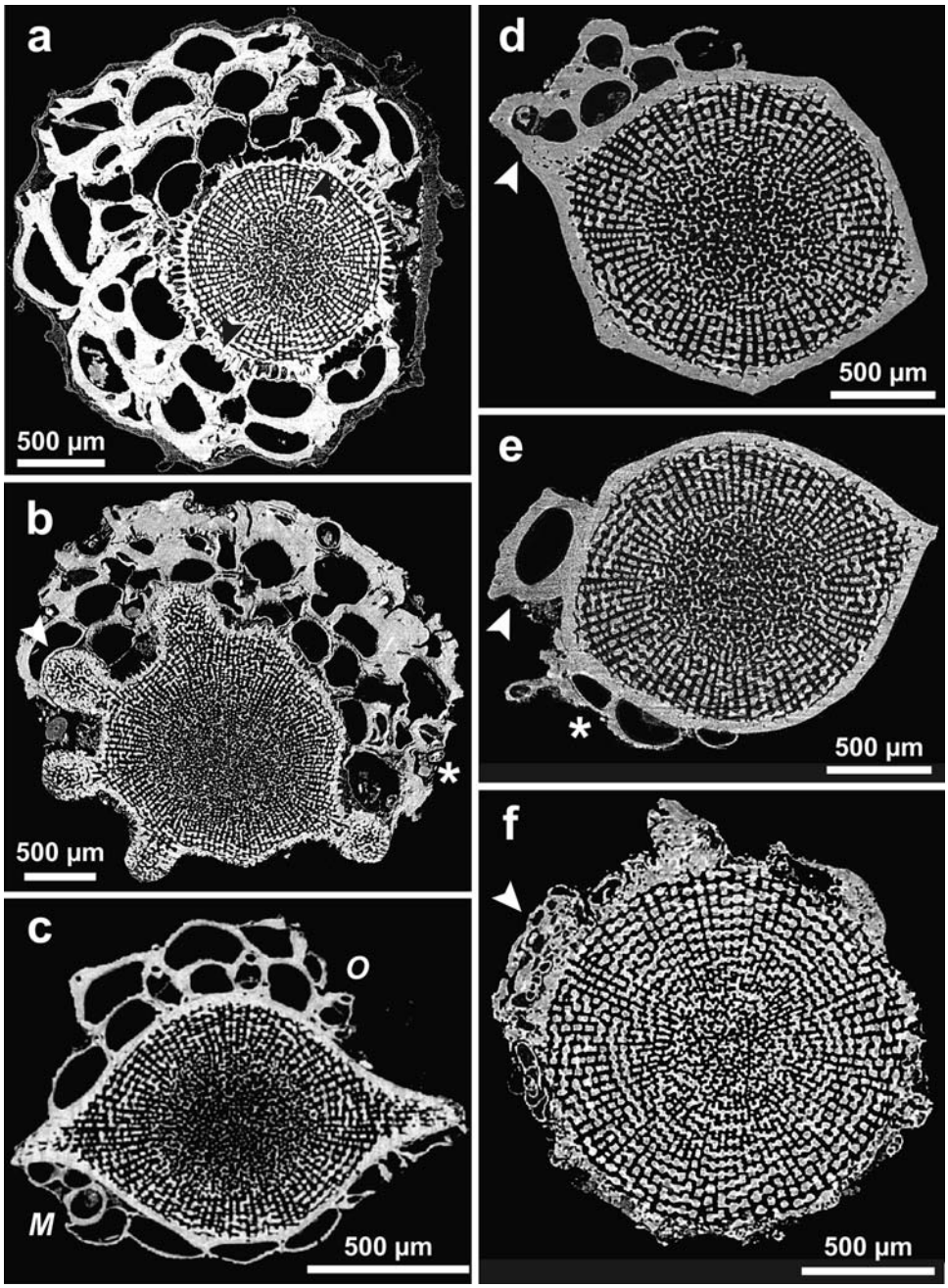

Fig. 4 Synchrotron µCT slices illustrating various ectosymbiont attachments by molding (**a**, **b**) and cementing (**c**–**f**) on cidaroid spines. **a** bryozoans with several layers of zooecia (*Osthimosia* sp. 1) on *Aporocidaris milleri*. The *black arrows* in the middle indicate places of perfect fit of the symbiont on the micropsines. **b** The same bryozoan on *Ctenocidaris speciosa*. The *arrow* on the left points to a close fit between the bryozoan and a thorn of the spine; the *asterisk* indicates symbionts stacking (see also Fig. 5c, d). **c**–**e** cementation of various symbionts on *Notocidaris lanceolata*: **c** *Micropora* sp. (*M*) and *Osthimosia* (*O*); **d** *Osthimosia* sp. 2 (the *arrow* shows a point of fusion between the bryozoan and the spine); **e** spirorbid worm (*arrow*) and bryozoan *Micropora* sp. (*asterisk*). **f** A cheilostomat bryozoan (*arrow*) on *Austrocidaris canaliculata*. Slices recorded at 17.4 keV and with a 2 K × 2 K CCD camera (**a**–**f** reconstructions with ~2.8 µm voxels)

for 73% of the total variance. The first axis is positively influenced by the maximal length of the spine and its basal and apical diameters, and negatively by the basal and apical spinosity. The detailed contribution of the parameters is given in supplementary table S2. Therefore, *C. perrieri* and *C. spinosa* mostly segregate from *C. speciosa* because they have smaller spines with larger thorns. Most of the differences are thus related to size, either directly (size of the spines and of their ornamentation) or indirectly through allometric effects.

Regarding the coverage by symbionts as approached by the criteria described above, the Mahalanobis distances among the three species are all significant, but the most similar coverages concern *C. perrieri* and *C. spinosa*, those between *C. speciosa* and *C. perrieri* being the most different (Table 3). Therefore, the observed morphological differences were also expressed in the way symbionts covered the spines.

Discussion

Taxonomic points

Species identifications in the cidaroid genus *Ctenocidaris* are somewhat difficult, but our µCT and SEM observations

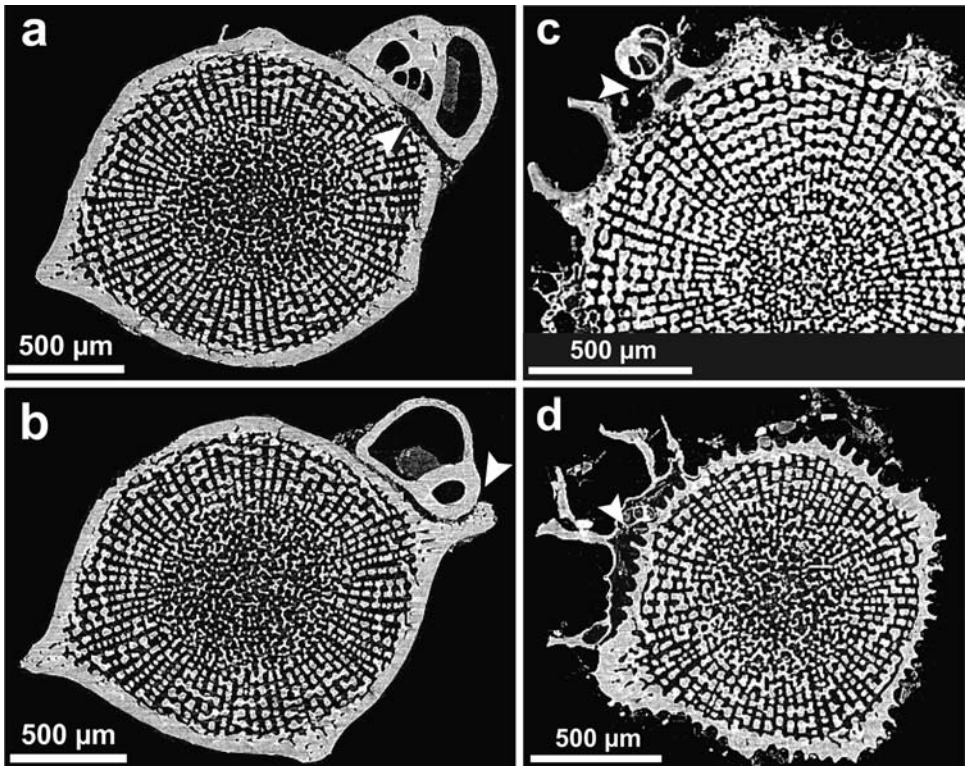

Fig. 5 Synchrotron µCT slices illustrating ectosymbionts corroding a cidaroid spine (**a**–**b**) and stacked one atop the others (**c**, **d**). **a**, **b** The foraminifer *Cibicides* sp. on *Notocidaris lanceolata* (*arrows* indicate places of corrosion of the cortex of the spine). The slices **a** and **b** are spaced by approximately 375 µm. **c** Foraminifer on a spirorbid in *A. canaliculata* (*arrow*). **d** Bryozoan on a foraminifer in *C. perrieri* (*arrow*) (**a**–**d** reconstructions with ~2.8 µm voxels)

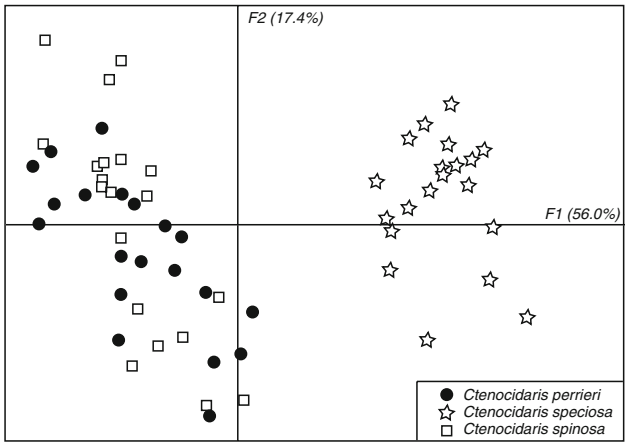

Fig. 6 Morphological variations of the apical spines of *C. perrieri*. *C. speciosa* and *C. spinosa*. Projection of the 60 analyzed apical spines on the two first axes of a factorial analysis performed on the 11 parameters listed on supplementary table S1

of spine shape and ornamentation have provided some clarification with respect to several species.

The combination of classical morphological characteristics and microstructural observations allowed us to assess the distinction between *C. perrieri*, *C. speciosa* and *C. spinosa*. These three species so far have been considered distinct, although with uncertainty based on their globiferous pedicellariae (David et al. 2005a). However, Fell (1976, p 237) wrote about *C. spinosa*: "In test and spine morphology there is a blending with *Ct. perrieri*". Then, he discussed

Table 3 Differences in coverage by symbionts between *Ctenocidaris perrieri*, *C. speciosa* and *C. spinosa*

	C. perrieri	*C. speciosa*	*C. spinosa*
C. perrieri		3.6813	1.1929
C. speciosa	$p = 0.0000$		1.8839
C. spinosa	$p = 0.0335$	$p = 0.0035$	

Mahalanobis distances (upper part of matrix) and their significance (lower part of matrix)

the strong external similarities in spine ornamentation: "The specimen […] had upper primaries with the spinules more or less regularly arranged, no different than many *Ct. perrieri*". Our morphometric approach confirms Fell's observations as *C. spinosa* and *C. perrieri* appear to overlap, while *C. speciosa* is distinct. However, the µCT identification of two categories of thorns allows discrimination of *C. perrieri*, strengthening the taxonomic distinctions among these three species. This confirms molecular results obtained from mitochondrial genes (COI and Cyt*b*) and supports the distinction between *C. perrieri* and *C. speciosa* (Lockhart unpublished data). The recorded microstructural difference demonstrates that there are two ways of constructing thorns in the genus *Ctenocidaris*. This is an exemplary case of adaptive convergence, particularly well expressed in the pair *C. perrieri* and *C. spinosa*. Indeed, the same morphological and functional structure (the thorn) is built in two different ways at the stereom scale. A similar

case of convergent evolution in cidaroids has recently been reported for the genus *Lissocidaris* in which the glossy aspect of the surface of primary spines in achieved by two distinct microstructural patterns (Coppard and van Noordenburg 2007). In addition, it is likely that the microstructures observed in *C. spinosa* and *C. speciosa* (thorns made of a dense thin cortex surrounding an internal labyrinthic stereom) correspond to an apomorphic expression of spines. Indeed, the diverse mesostructural ornamentations of cidaroid spines (bumps, thorns, etc.) are generally formed by the cortex layer alone (Mortensen 1928; Fell 1954; Märkel and Röser 1983a). An appropriate robust answer will only come from further molecular investigation (Lockhart et al. 2003), but this suggests that *C. speciosa* and *C. spinosa* might be derived sister species within the clade Ctenocidarinae.

Convergent expressions of mesostructures seem rather common within Ctenocidarinae. In *Rhynchocidaris triplopora*, the coalescence of large acuminate spikes, derived from the cortex layer, likely represents a third way of forming thorns. Another case of convergence, although to a lesser extent, concerns longitudinal ridges, which are expressed as folded thickenings of a cavernous cortex in *Austrocidaris canaliculata*, while they are formed by the coalescence of coarse microspines in *Notocidaris hastata*. The coalescence of microspines was also the basis for the convergence observed in *Lissocidaris xanthe* (Coppard and van Noordenburg 2007). The multiplicity of such examples suggests that the coalescence of microstructures might be a standard path leading to convergent mesostructures. This in turn means that mesostructures alone are not reliable taxonomic characters without knowledge of the microstructure.

At the scale of Ctenocidarinae, much of primary spine diversity comes from variations in the way the cortex layer is expressed: smooth in *N. lanceolata*, granulose in *C. rugosa*, spiny in *C. perrieri*. Even in species formerly considered very close, microstructural characters provide additional criteria allowing one to ascertain differences. For example, *C. geliberti* and *C. rugosa*, distinguished by the degree to which the spines are ornamented by bumps, have sometimes been synonymized (Mortensen 1928). Actually, μCT shows that they also differ in microspine shape, fused at their top in *C. geliberti* and disconnected in *C. rugosa*, thereby confirming their status as separate species.

Microspines and the parasite *Echinophyces mirabilis*

The nature of some microstructures is somewhat difficult to assess. Our μCT observations have demonstrated that the fine filaments of *Rhynchocidaris triplopora* were actually part of the stereom. Several other species bear microspines that correspond to expanded stereom trabeculae more or less densely coating the spine. Various degrees of "microspinosity" are expressed. Microspines are totally lacking in *Notocidaris lanceolata*, they are small in *Apocidaris milleri* or *Ctenocidaris rugosa*, and they are large in *C. perrieri* or *C. spinosa*. *Rhynchocidaris triplopora* departs strongly from all other species in having very thin filaments extending from and around the spine. Observed connections between those filaments and the cortex of the spine, as well as their aspect in μCT, suggest that they are calcite extensions of the cortex. Therefore, the fuzzy aspect of *R. triplopora* spines has to be regarded as a microstructural characteristic. In addition, the microspine differences between *R. triplopora* and the other species (e.g. *C. spinosa*) are more a matter of degree.

Therefore, bundles of microspines in *R. triplopora* are just one extreme in the range of microspinosity. This, in turn, casts some doubt on their putative, but long-standing, interpretation as microparasites (Mortensen 1909, 1910; Mortensen and Rosenvinge 1910; David et al. 2005a). Indeed, Mortensen (1909) considered that the hairy aspect of the cortex of primary spines of *R. triplopora* was due to *Echinophyces mirabilis*, a microorganism living in the stereom of the spines, which was tentatively identified as a fungus. It has also been reported in *C. speciosa* (Mortensen 1910), and *C. perrieri* (Koehler 1912), and it was considered to be a parasite mysteriously inducing extensive morphological transformations, particularly in the reproductive system. Recently, Lockhart (unpubl. molecular data from 18S ribosomal gene) demonstrated that the specimens with "transformed" morphologies—formerly attributed to the effect of the parasite—were actually not phylogenetically related to "normal" specimens of their respective species, but to each other. Consequently, she erected the genus *Miracidaris* to gather those "transformed" specimens, casting doubt upon the supposed effects of *E. mirabilis*. Our microstructural observations, showing that the filaments are part of the spine cortex, challenge the parasitic interpretation of filaments, and confirm Lockhart's results. However, this new interpretation, which is specific for *R. triplopora*, cannot be generalized. Indeed, Lockhart has also clearly said that *E. mirabilis* exists and is a symbiont (putatively a parasite) on the primary spines of representatives of several species. The question of *E. mirabilis* affiliation is still open, but Lockhart proposed to assign it to the Orthonectida, a poorly known phylum of parasites (Hanelt et al. 1996).

Adaptive significance of symbiont attachments

Cidaroid spines display various meso- and microstructures that probably affect the settlement of ectosymbionts. We have shown that there is equivocal relationship between a type of structure and a mode of attachment. This raises a question about the adaptive significance of symbiont attachments.

As early as 1928, Mortensen posed the question of whether the symbionts settled on cidaroid spines were parasitic. Answering the question is very complex. First, it would be necessary to check if specimens bearing more symbionts have reduced fitness. In addition, several species of organisms can settle on a single cidaroid specimen, but the load represented by each symbiont species alone might not be sufficient to create a handicap. The situation reminds one of "Murder on the Orient Express"; there are several perpetrators, not a single culprit. As expressed by Mortensen, the total burden creates the handicap. Therefore, each species could contribute to a "collective parasitism" without being strictly a parasite by itself. This potential "collective parasitism" corresponds to a peculiar case that could be compared with microbial pathogens or epiphytic communities. More specifically, parasitism is strongly suspected in the case of the foraminifer *Cibicides* sp. that corrodes the spines of *N. lanceolata*. This hypothesis is strengthened by the established parasitism of *Cibicides refulgens*, also from Antarctica, which is known to erode calcareous substrates such as scallop shells (Alexander and Delaca 1987).

Consider that the attachment of ectosymbionts represents a cost for the cidaroids and an advantage for the settlers (most symbionts are filter feeders, which gain better access to the water column when fixed on spines). How, then, do ectosymbionts benefit or not from the micro- and mesostructures of the spines? How can the cidaroids avoid symbiont overload on spines? Is autotomy of the primary spines an appropriate adaptive mechanism? If so, the cost of growing a new spine has to be compared with the handicap generated by the ectosymbiont load. Are microstructures a way to prevent strong attachment of symbionts or the settlement of post-larval stages? Some symbionts are apparently unable to match the complexity of the microstructures, and so are only loosely attached in discontinuous spots. In this way, the bundles of filaments of *R. triplopora* are likely to be effective as only 20% of *R. triplopora* spines have more than 25% coverage (Hétérier et al. 2004). On the other hand, some symbionts benefit from the microstructures and obtain firmer anchorage. This is the case for the bryozoan on *A. milleri*, which holds onto the spine using the microspines. Microspines of *C. speciosa* and *C. spinosa* are rather similar and less sharp and dense than those of *C. perrieri*. However, the symbiont diversity is not statistically different for *C. perrieri* and *C. spinosa*, while it is significantly lower for *C. speciosa* (Hétérier pers. comm.). Therefore, there is no clear relationship between the development of microstructures and the attachment of ectosymbionts. Regarding the mesostructures, it seems unambiguous that the most ornamented spines are ordinarily the most colonized. This likely eliminates them as a defense against ectosymbiont attachments.

To conclude, our study suggests that there is no universal mechanism allowing cidaroids to deal with ectosymbionts. Hence, detailed investigations taking into account the ectosymbiont specificity to some hosts will be necessary to clarify their parasitic nature, including appraisal of the costs or benefits of such relationships, or of the antifouling role of stereom trabeculae. Because it is non-destructive, there is no doubt that microtomography will be employed in the future to explore the physical relationships between cidaroids and the ectosymbionts colonizing their spines.

Acknowledgments This work is part of the BIANZO I and II projects supported by the Belgian Science Policy (PADDII projects). VH was supported by a PhD grant from the Belgian Science Policy (Belspo). This paper is a contribution of the team «Forme, Evolution, Diversité» of the laboratory Biogéosciences and of the Centre interuniversitaire de Biologie marine. It also contributes to the Agence Nationale de la Recherche project ANTFLOCKS. Use of the Advanced Photon Source at Argonne National Laboratory was supported by the US Department of Energy, Office of Science, Office of Basic Energy Sciences, under Contract No. DE-AC02-06CH11357.

References

Alexander SP, Delaca TE (1987) Feeding adaptation of the foraminiferan *Cibicides refulgens* living epizoically and parasitically on the Antarctic scallop *Adamussium colbecki*. Biol Bull 173:136–159. doi:10.2307/1541868

Alvarado JJ (2008) Seasonal occurrence and aggregation behavior of the sea urchin *Astropyga pulvinata* (Echinodermata: Echinoidea) in Bahia Culebra, Costa Rica. Pac Sci 62:579–592. doi:10.2984/1534-6188(2008)62[579:SOAABO]2.0.CO;2

Bailey RC, Byrnes J (1990) A new, old method for assessing measurement error in both univariate and multivariate morphometric studies. Syst Zool 39:124–130. doi:10.2307/2992450

Coppard SE, van Noordenburg H (2007) A new species of *Lissocidaris* (Echinodermata: Echinoidea: Cidaridae) from the Philippines: convergent evolution among smooth-spined cidaroids. Zootaxa 1493:53–65

David B, Mooi R (1999) Contributions of the extraxial-axial theory to understanding the echinoderms. Bull Soc Geol Fr 170:91–101

David B, Choné T, Mooi R, De Ridder C (2005a) Antarctic Echinoidea. In: Synopses of the Antarctic benthos, vol 10. Koeltz Scientific Books, Königstein

David B, Choné T, Festeau A, Mooi R, De Ridder C (2005b) Biodiversity of Antarctic echinoids: a comprehensive and interactive database. Sci Mar 69(Suppl. 2):201–203. doi:10.3989/scimar.2005.69s2201

Fell HB (1954) Tertiary and recent Echinoidea of New Zealand. NZ Geol Surv Paleontol Bull 23:1–62

Fell FJ (1976) The Cidaroida (Echinodermata: Echinoidea) of Antarctica and the Southern oceans. PhD thesis, University of Maine, Orono

Gutt J, Schickan T (1998) Epibiotic relationships in the Antarctic benthos. Antarct Sci 10:398–405. doi:10.1017/S0954102098000480

Hanelt B, Van Schyndel D, Adema CM, Lewis LA, Loker ES (1996) The phylogenetic position of *Rhopaluva ophiocomae* (Orthonectida) based on 18 s ribosomal DNA sequence analysis. Mol Biol Evol 13:1187–1191

Hétérier V, De Ridder C, David B, Rigaud T (2004) Comparative biodiversity of ectosymbionts in two Antarctic cidarid echinoids,

Ctenocidaris spinosa and *Rhynchocidaris triplopora*. In: Heinzeller T, Nebelsick JH (eds) Echinoderms: München. Taylor and Francis, London, pp 201–205

Hétérier V, David B, De Ridder C, Rigaud T (2008) Ectosymbiosis, a critical factor in establishing local benthic biodiversity in Antarctic deep sea. Mar Ecol Prog Ser 364:67–76. doi:10.3354/meps07487

Koehler R (1912) Echinodermes (astéries, ophiures et échinides). In: 2ème Expédition Antarctique Française 1908–1910. Masson, Paris

Linse K, Walker LJ, Barnes DKA (2008) Biodiversity of echinoids and their epibionts around the Scotia Arc, Antarctica. Antarct Sci 20:227–244. doi:10.1017/S0954102008001181

Lockhart SJ, Mooi RJ, Pearse JS (2003) Phylogeny, reproductive mode, and parasitism in Antarctic cidaroid sea urchins. Ber Polar Meeresforsch 470:112–115

Märkel K, Röser U (1983a) The spine tissues in the echinoid *Eucidaris tribuloides*. Zoomorphology 103:25–41. doi:10.1007/BF00312056

Märkel K, Röser U (1983b) Calcite resorption in the spine of the Echinoid *Eucidaris tribuloides*. Zoomorphology 103:43–58. doi:10.1007/BF00312057

Mooi R, David B (1998) Evolution within a bizarre phylum: homologies of the first echinoderms. Am Zool 38:965–974. doi:10.1093/icb/38.6.965

Mooi R, David B, Fell FJ, Choné T (2000) Three new species of bathyal cidaroids (Echinodermata: Echinoidea) from the Antarctic region. Proc Biol Soc Wash 113:224–237

Mortensen T (1909) Die Echinoiden der Deutschen Südpolar Expedition 1901-1903. In: Deutsche Südpolar Expedition. Reimer, Berlin

Mortensen T (1910) The Echinoidea of the Swedish South Polar Expedition. In: Schwedische Südpolar Expedition 1901–03, vol 6. Lithographisches Institut des Generalstabs, Stockholm

Mortensen T (1928) A monograph of the Echinoidea, vol 1 Cidaroidea. Reitzel, Copenhagen

Mortensen T, Rosenvinge KL (1910) Sur quelques plantes parasites dans les échinodermes. K Dan Vidensk Selsk Forhandling 4:339–354

Smith AB (1980) Stereom microstructure of the echinoid test. Palaeontological Association, Spec Pap Palaeontol 25

Vaitilingon D, Eeckhaut I, Fourgon D, Jangoux M (2004) Population dynamics, infestation and host selection of *Vexilla vexillum*, an ectoparasitic muricid of echinoids, in Madagascar. Dis Aquat Organ 61:241–255. doi:10.3354/dao061241

Wang Y, De Carlo F, Mancini D, McNulty I, Tieman B, Bresnahan J, Foster I, Insley J, Lane P, von Laszewski G, Kesselman C, Su MH, Thiebaux M (2001) High-throughput X-ray microtomography system at the Advanced Photon Source. Rev Sci Instrum 72:2062–2068. doi:10.1063/1.1355270